A positive-weight next-to-leading-order Monte Carlo for e^+e^- annihilation to hadrons

Oluseyi Latunde-Dada and Bryan Webber

Cavendish Laboratory, University of Cambridge,
JJ Thomson Avenue, Cambridge CB3 0HE, U.K.
E-mail: seyi@hep.phy.cam.ac.uk,webber@hep.phy.cam.ac.uk

Stefan Gieseke

Institut für Theoretische Physik, Universität Karlsruhe.
76128 Karlsruhe, Germany.
E-mail: gieseke@particle.uni-karlsruhe.de

ABSTRACT: We apply the positive-weight Monte Carlo method of Nason for simulating QCD processes accurate to Next-To-Leading Order to the case of e^+e^- annihilation to hadrons. The method entails the generation of the hardest gluon emission first and then subsequently adding a 'truncated' shower before the emission. We have interfaced our result to the `Herwig++` shower Monte Carlo program and obtained better results than those obtained with `Herwig++` at leading order with a matrix element correction.

Contents

1. Introduction

Matching next-to-leading order (NLO) calculations to shower Monte Carlo (SMC) models is highly non-trivial. One method (MC@NLO) has been proposed in [1] and has been successfully applied to several processes [2, 3] in connection with the FORTRAN HERWIG parton shower. One drawback of the method is the generation of negative weighted events which are unphysical.

An alternative method proposed in [4] overcomes the negative weight problem. It has successfully been applied to Z pair hadroproduction [5] and involves the generation of the hardest radiation independently of the SMC model used to generate the parton shower. To preserve the soft radiation distribution, the addition of a 'truncated shower' of soft coherent radiation before the hardest emission is necessary. In this report, we will be implementing this method for electron-positron annihilation to hadrons at a centre-of-mass energy of 91.2 GeV. The SMC we will be employing is Herwig++,[6] which will perform the rest of the showering, hadronization and decays.

In section 2, we discuss the generation of the hardest emission according to the matrix element via a modified Sudakov form factor. In section 3, we go on to describe the generation of a simplified form of the 'truncated' shower. We determine the probability for the emission of at most one gluon before the hardest emission and re-shuffle the momenta of the outgoing particles accordingly. This is a reasonable first approximation since the probability of emitting an extra gluon is small.

In section 4, we present our results compared with the measured data and those obtained using Herwig++ with a matrix element correction. Finally in section 5, we summarize our conclusions.
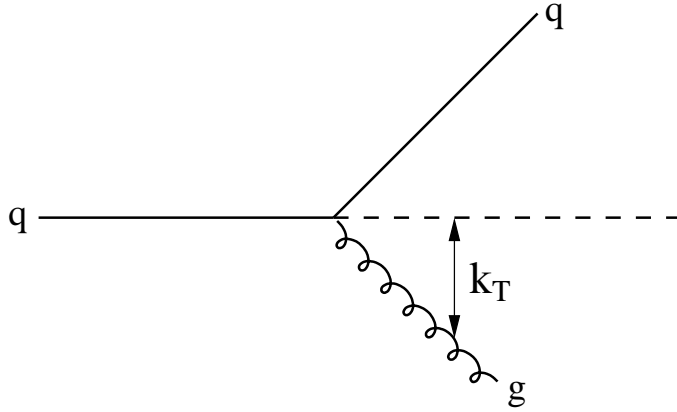
Figure 1: Transverse momentum, k_T.

2. Hardest emission generation

2.1 Hardest emission cross section

The order-α_s differential cross section for the process $e^+e^- \to q\bar{q}g$, neglecting the quark masses, can be written as

$$R(x,y) = \sigma_0 W(x,y) = \sigma_0 \frac{2\alpha_s}{3\pi} \frac{x^2 + y^2}{(1-x)(1-y)} \tag{2.1}$$

where σ_0 is the Born cross section, $W = R/\sigma_0$, x and y are the energy fractions of the quark and antiquark and $2 - x - y$ is the energy fraction of the gluon. R has collinear singularities when the quark or antiquark is aligned with the gluon. When combined with the virtual corrections, these singularities can be integrated to give the well known total cross section to order-α_s,

$$\sigma_{\text{NLO}} = \sigma_0 \left[1 + \frac{\alpha_s}{\pi}\right] . \tag{2.2}$$

From [4], we can write the cross section for the hardest gluon emission event as

$$d\sigma = \sum \bar{B}(v) d\Phi_v \left[\Delta_R^{(NLO)}(0) + \Delta_R^{(NLO)}(p_T)\frac{R(v,r)}{B(v)}d\Phi_r\right] \tag{2.3}$$

where $B(v)$ is the Born cross section and v is the Born variable, which in this case is the angle θ between the e^+e^- beam axis and the $q\bar{q}$ axis. r represents the radiation variables (x and y for our specific case), $d\Phi_v$ and $d\Phi_r$ are the Born and real emission phase spaces respectively.

$\Delta_R^{\text{NLO}}(p_T)$ is the modified Sudakov form factor for the hardest emission with transverse momentum p_T, as indicated by the Heaviside function in the exponent of (2.4),

$$\Delta_R^{\text{NLO}}(p_T) = \exp\left[-\int d\Phi r \frac{R(v,r)}{B(v)}\Theta(k_T(v,r) - p_T)\right] . \tag{2.4}$$

Furthermore,

$$\bar{B}(v) = B(v) + V(v) + \int (R(v,r) - C(v,r))d\Phi_r . \tag{2.5}$$
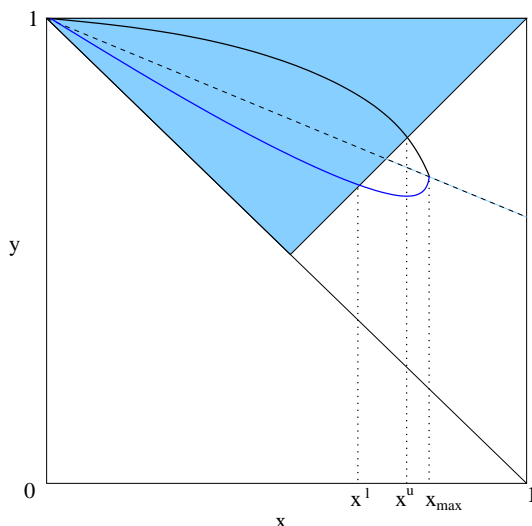
Figure 2: Phase space and y solutions for $\kappa < 0.08333$ in the region $x > y$.
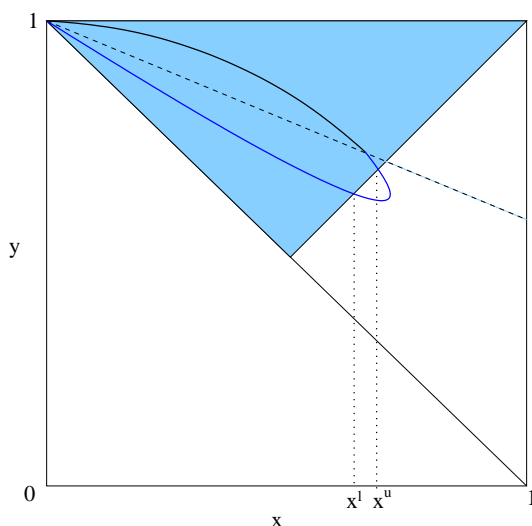

Figure 3: Phase space and y solutions for $\kappa > 0.08333$ in the region $x > y$.

$\bar{B}(v)$ is the sum of the Born, $B(v)$, virtual, $V(v)$ and real, $R(v,r)$ terms, (with some counter-terms, $C(v,r)$). It overcomes the problem of negative weights since in the region where $\bar{B}(v)$ is negative, the NLO negative terms must have overcome the Born term and hence perturbation theory must have failed.

Now explicitly for e^+e^- annihilation,

$$\Delta_R^{\mathrm{NLO}}(p_T) = \exp\left[-\int dx\,dy \frac{2\alpha_s}{3\pi} \frac{x^2 + y^2}{(1-x)(1-y)} \Theta(k_T(x,y)) - p_T\right] \qquad (2.6)$$

where x and y are the energy fractions of the quark and antiquark and we define

$$k_T(x,y) = \sqrt{s \frac{(1-x)(1-y)(x+y-1)}{\max(x,y)^2}} \qquad (2.7)$$

and s as the square of the center-of-mass energy. k_T is the transverse momentum of the hardest emitted gluon relative to the splitting axis, as illustrated in figure 1.

2.2 Generation of radiation variables, x and y

From (2.1) and (2.3), it can be deduced that the radiation variables are to be generated according to the probability distribution

$$\Delta^W(k_T)W(x,y)dx\,dy \tag{2.8}$$

where in the particular case of e^+e^- annihilation, $\Delta^W(k_T)$ and $W(x,y)$ are given in (2.6) and (2.1) respectively. However for ease of integration, we will use a function

$$U(x,y) = \frac{2\alpha_s}{3\pi} \frac{2}{(1-x)(1-y)} \geq W(x,y) \tag{2.9}$$

in place of $W(x,y)$. As we shall see later, the true distribution is recovered using the veto technique. The variables x and y are then generated according to

$$\Delta^U(k_T)U(x,y) = U(x,y)\exp\left[-\int U(x,y)\Theta(k_T(x,y)-p_T)dx\,dy\right] . \tag{2.10}$$

This is outlined in the following steps:

i) Set $p_{\max} = k_{T\max}$.

ii) For a random number, n between 0 and 1, solve the equation below for p_T

$$n = \frac{\Delta^U(p_T)}{\Delta^U(p_{\max})} . \tag{2.11}$$

iii) Generate the variables x and y according to the distribution

$$U(x,y)\delta(k_T(x,y)-p_T) . \tag{2.12}$$

iv) Accept the generated value of p_T with probability W/U. If the event is rejected set $p_{\max} = p_T$ and go to step ii).

Now for e^+e^- annihilation,

$$\int U(x,y)\Theta(k_T(x,y)-p_T)dx\,dy = \int_0^1 dx \int_{1-x}^1 dy U(x,y)\Theta(k_T(x,y)-p_T) . \tag{2.13}$$

In the region where $x > y$, let's define the dimensionless variable, κ as

$$\kappa = \frac{k_T^2}{s} = \frac{(1-x)(1-y)(x+y-1)}{x^2} . \tag{2.14}$$

There are 2 solutions for y for each value of x and κ, i.e $y_1 = y$ and $y_2 = 2 - x - y$.

$$y_{1,2} = \frac{-2 + 3x - x^2 \mp \sqrt{x^2 - 2x^3 + x^4 - 4\kappa x^2 + 4\kappa x^3}}{2(x-1)} . \tag{2.15}$$

Exchanging the y variable for κ in (2.13) we find

$$\int U(x,y)\Theta(k_T(x,y)-p_T)dxdy = \int_{x_{\min}}^{x_{\max}} dx \int_{\kappa}^{\kappa_{\max}} d\kappa \frac{2\alpha_s(\kappa s)}{3\pi} \frac{dy}{d\kappa} U(x,\kappa)$$
$$= \int_{x_{\min}}^{x_{\max}} dx \int_{\kappa}^{\kappa_{\max}} d\kappa \frac{2\alpha_s(\kappa s)}{3\pi} \frac{4}{(1-x+\rho(\kappa,x))\rho(\kappa,x)}$$

(2.16)

where

$$\rho(\kappa,x) = \sqrt{(1-x)(1-4\kappa-x)}\,.$$

(2.17)

Note that the argument of α_s is the scale $k_T{}^2 = \kappa s$ with $\Lambda_{\rm QCD} = 200\,{\rm MeV}$. Equation (2.16) applies to the region of phase space where $x > y$. For the region $x < y$, x and y are exchanged in the equation.

The x integration can be performed to yield

$$\int U(x,y)\Theta(k_T(x,y)-p_T)dxdy = \int_{\kappa}^{\kappa_{\max}} d\kappa \frac{2\alpha_s(\kappa s)}{3\pi} \left[\frac{\ln(1-x)}{\kappa} + \right.$$
$$\left. + \frac{2\ln(\sqrt{1-x}+\sqrt{1-4\kappa-x})}{\kappa} \right]_{x_{\min}}^{x_{\max}}$$

(2.18)

For $\kappa \leq 0.08333$, the region of phase space where $x > y$ and the two solutions for y for given values of x and κ are illustrated in figure 2.

The two solutions lie on either side of the dashed line $y = 1 - \frac{1}{2}x$ and are equal when $x = x_{\max} = 1 - 4\kappa$ which lies on the dotted line. At $\kappa = 0.08333$, the branches meet along the line $y = x$ and there is only one solution for y in the region (the lower branch). So for $\kappa > 0.08333$, only one y solution exists. In addition there are no y solutions for $\kappa > 0.09$. This is illustrated in figure 3.

Also note that for $x < x^u$, there is only one solution for y.

In the region where there are two solutions, the integral in (2.18) is performed along both branches independently and summed. For the upper branch, x runs from x^u to $x_{\max} = 1 - 4\kappa$ while for the lower branch, x runs from x^l to $x_{\max}$ where if we define

$$x_a = 39\kappa - 1 + \kappa^3 + 15\kappa^2\,,$$
$$x_b = 6\sqrt{-33\kappa^2 + 3\kappa - 3\kappa^3}\,,$$
$$x_c = \sqrt{x_a{}^2 + x_b{}^2}\,,$$
$$x_d = \tan^{-1}\left(\frac{x_b}{x_a}\right)\,,$$
$$x_e = -\frac{1}{12}x_c^{\frac{1}{3}}\cos\left(\frac{x_d}{3}\right)\,,$$
$$x_f = \frac{(-1-\kappa^2-10\kappa)\cos\left(\frac{x_d}{3}\right)}{12x_c^{\frac{1}{3}}}\,,$$
$$x_g = \frac{\kappa+5}{6}\,,$$
$$x_h = \frac{\sqrt{3}}{12}\sin\left(\frac{x_d}{3}\right)\left(x_c^{\frac{1}{3}} + \frac{1+\kappa^2+10\kappa}{x_c^{\frac{1}{3}}}\right)\,,$$

(2.19)

we can write x^u and x^l as;

$$x^u = x_e + x_f + x_g + x_h \,,$$
$$x^l = x_e + x_f + x_g - x_h \,; \tag{2.20}$$

In the region where there is only one solution for y, x runs from x^l to x^u.

The κ integration can then be performed numerically. Having performed the integration, values for κ and hence k_T are then generated according to steps 1 and 2 in section 2.2. In step 3 of section 2.2, the variables x and y are to be distributed according to $U(x,y)\delta(k_T(x,y) - p_T)$. This is the subject of the next section.

2.3 Distributing x and y according to $U(x,y)$

To generate x and y values with a distribution proportional to $U(x,y)\delta(k_T(x,y) - p_T)$, we can use the δ-function to eliminate the y variable by computing

$$D(x) = \int \delta(k_T - p_T) U(x,y) = \left. \frac{U(x,y)}{\frac{\partial k_T}{\partial y}} \right|_{y=\bar{y}} \tag{2.21}$$

where $\bar{y}$ is such that $k_T(x,\bar{y}) = p_T$. Note that $\frac{\partial k_T}{\partial y}$ is the same for both y solutions. We then generate x values with a probability distribution proportional to D with hit-and-miss techniques as described below. All events generated have uniform weights.

  i) Randomly sample x, N_x times (we used $N_x = 10^5$) in the range $[x_{\min} : x_{\max}]$ for the selected value of κ.

 ii) For each value of x, evaluate $\bar{D} = D(x,y_1) + D(x,y_2)$ if there are two solutions for the selected κ and $\bar{D} = D(x,y_2)$ if there is only one solution. Also, if $\kappa < 0.08333$ and $x < x^u$ (see figure 2), there is only one y solution so evaluate $\bar{D} = D(x,y_2)$.

iii) Find the maximum value $\bar{D}_{\max}$ of $\bar{D}$ for the selected value of κ from the set of N_x points that have been sampled.

 iv) Next, select a value for x in the allowed range and evaluate $\bar{D}$.

  v) If $\bar{D} > r\bar{D}_{\max}$ (where r is a random number between 0 and 1), accept the event, otherwise go to iv) and generate a new value for x.

 vi) If for the chosen value of x, there are two solutions for y, select a value for y in the ratio $D(x,y_1) : D(x,y_2)$.

vii) Compare $U(x,y)$ with the true matrix element, $W(x,y)$. If the event fails this veto, set $\kappa_{\max} = \kappa$ and regenerate a new κ value as discussed in section 2.2.

Particle	Experiment	Measured	`Herwig++` ME	Nason@NLO
All Charged	M,A,D,L,O	20.924 ± 0.117	20.9157	21.117
γ	A,O	21.27 ± 0.6	23.02	22.80
π^0	A,D,L,O	9.59 ± 0.33	10.44	10.45
$\rho(770)^0$	A,D	1.295 ± 0.125	1.201	1.19
$\pi^\pm$	A,O	17.04 ± 0.25	17.28	17.36
$\rho(770)^\pm$	O	2.4 ± 0.43	1.94	1.85
η	A,L,O	0.956 ± 0.049	0.976	1.02
$\omega(782)$	A,L,O	1.083 ± 0.088	0.851	0.745
$\eta'(958)$	A,L,O	0.152 ± 0.03	0.138	0.084
K^0	S,A,D,L,O	2.027 ± 0.025	1.949^*	2.742^*
$K^*(892)^0$	A,D,O	0.761 ± 0.032	0.627^*	0.713
$K^*(1430)^0$	D,O	0.106 ± 0.06	0.084	0.033
$K^\pm$	A,D,O	2.319 ± 0.079	2.155	2.259
$K^*(892)^\pm$	A,D,O	0.731 ± 0.058	0.614	0.699
$\phi(1020)$	A,D,O	0.097 ± 0.007	0.116	0.101
p	A,D,O	0.991 ± 0.054	0.871	0.958
Δ^{++}	D,O	0.088 ± 0.034	0.085	0.086
Σ^-	O	0.083 ± 0.011	0.0711	0.073
Λ	A,D,L,O	0.373 ± 0.008	0.391	0.030
Σ^0	A,D,O	0.074 ± 0.009	0.091	0.097
Σ^+	O	0.099 ± 0.015	0.077	0.089
$\Sigma(1385)^\pm$	A,D,O	0.0471 ± 0.0046	0.0307^*	0.031
Ξ^-	A,D,O	0.0262 ± 0.001	0.032^*	0.034^*
$\Xi(1530)^0$	A,D,O	0.0058 ± 0.001	0.0092^*	0.0096^*
Ω^-	A,D,O	0.00125 ± 0.00024	0.00197	0.00194
$f_2(1270)$	D,L,O	0.168 ± 0.021	0.164	0.173
$f_2'(1525)$	D	0.02 ± 0.008	0.0146	0.0184
$D^\pm$	A,D,O	0.184 ± 0.018	0.252^*	0.282^*
$D^*(2010)^\pm$	A,D,O	0.182 ± 0.009	0.173	0.185
D^0	A,D,O	0.473 ± 0.026	0.497	0.497
$D_s^\pm$	A,O	0.129 ± 0.013	0.130	0.150
$D_s^{*\pm}$	O	0.096 ± 0.046	0.06	0.044
J/Ψ	A,D,L,O	0.00544 ± 0.00029	0.00349^*	0.0033^*
Λ_c^+	D,O	0.077 ± 0.016	0.0215^*	0.0303^*
$\Psi'(3685)$	D,L,O	0.00229 ± 0.00041	0.00165	0.00154

Table 1: Multiplicities per event at 91.2 GeV. We show results from `Herwig++` with a matrix element correction (Herwig++ ME) and the new method, Nason@NLO . Experiments are Aleph(A), Delphi(D), L3(L), Opal(O), Mk2(M) and SLD(S). The $*$ indicates a prediction that differs from the measured value by more than three standard deviations. Data are combined and updated from a variety of sources, see ref [10].

N.B.: For the region $y > x$, exchange x and y in the above discussion. In this way, the smooth phase space distribution in figure 4 below was obtained for the hardest emission events. The plot show 2,500 of these events.

3. Adding the truncated shower

As mentioned in section 1, a 'truncated shower' would need to be added before the hardest emission to simulate the soft radiation distribution. Due to angular ordering, the 'trun-
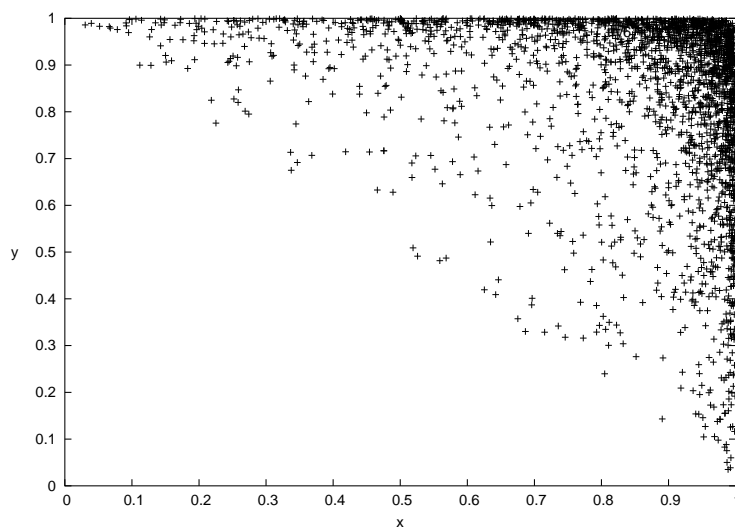
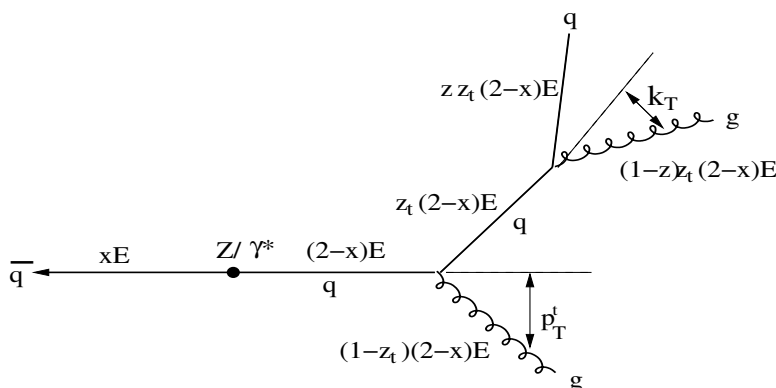**Figure 4:** Phase space and distribution of hardest emissions.

Figure 5: Adding the 'truncated' emission. ($E = 45.6\,\text{GeV}$)

cated' radiation is emitted at a wider angle than the angle of the hardest emission as well as a lower p_T. This means the 'truncated' radiation does not appreciably degrade the energy entering the hardest emission and justifies our decision to generate the hardest emission first.

Below is an outline of how the 'truncated shower' was generated. We will consider the case in which at most one extra gluon is emitted by the quark or antiquark before the hardest emission. The outline closely follows the `Herwig++` parton shower evolution method described in [6, 7] where the evolution variables z, the momentum fractions, and $\tilde{q}$, the evolution scale, determine the kinematics of the shower.

i) Having generated the p_T of the hardest emission and the energy fractions x and y, calculate the momentum fraction z and $1 - z$ of the partons involved in the hardest emission. We will assume henceforth that $x > y$ and that y is the energy fraction of

the quark, i.e. the quark is involved in the hardest emission. Then

$$z = \frac{y}{2-x} \tag{3.1}$$

where as defined above z and $1-z$ are the momentum fractions of the quark and gluon respectively.

ii) Next generate the momentum fraction z_t of the 'truncated' radiation according to the splitting function $P_{qq} = \frac{1+z^2}{1-z}$ within the range

$$\frac{\mu}{\tilde{q}_i} < z_t < 1 - \frac{Q_g}{\tilde{q}_i} \tag{3.2}$$

where $\tilde{q}_i$ is the initial evolution scale, i.e. $\sqrt{s} = 91.2\,\text{GeV}$, $\mu=\max(m_a, Q_g)$, m_a is the mass of the quark and Q_g is a cutoff introduced to regularize soft gluon singularities in the splitting functions. In this report, a Q_g value of $0.75\,\text{GeV}$ (and hence $\mu = 0.75\,\text{GeV}$) was used. z_t is the momentum fraction of the quark after emitting the 'truncated' gluon with momentum fraction $1 - z_t$.

iii) Having generated a value for z_t, determine the scale $\tilde{q}_h$ of the hardest emission from

$$\tilde{q}_h = \sqrt{\frac{p_T{}^2}{z^2(1-z)^2} + \frac{\mu^2}{z^2} + \frac{Q_g{}^2}{z(1-z)^2}} \tag{3.3}$$

where $z = z_t$.

iv) Starting from an initial scale $\tilde{q}_i$, the probability of there being an emission next at the scale $\tilde{q}$ is given by

$$S(\tilde{q}_i, \tilde{q}) = \frac{\Delta(\tilde{q}_c, \tilde{q}_i)}{\Delta(\tilde{q}_c, \tilde{q})} \tag{3.4}$$

where

$$\Delta(\tilde{q}_c, \tilde{q}) = exp\left[-\int_{\tilde{q}_c}^{\tilde{q}} \frac{d\tilde{q}^2}{\tilde{q}^2} \int dz \frac{\alpha_s}{2\pi} P_{qq} \Theta(0 < p_T^t < p_T)\right]. \tag{3.5}$$

$\tilde{q}_c$ is the lower cutoff of the parton shower which was set to $0.4\,\text{GeV}$ in this report, α_s is the running coupling constant evaluated at $z(1-z)\tilde{q}$, P_{qq} is the $q \to qg$ splitting function and k_T is the transverse momentum of the hardest emission. The Heaviside function ensures that the transverse momentum, p_T^t of the truncated emission is real and is less than p_T. To evaluate the integral in (3.5), we overestimate the integrands and apply vetoes with weights as described in [6]. With r a random number between 0 and 1, we then solve the equation

$$S(\tilde{q}_i, \tilde{q}) = r \tag{3.6}$$

for $\tilde{q}$. If $\tilde{q} > \tilde{q}_h$, the event has a 'truncated' emission. If $\tilde{q} < \tilde{q}_h$, there is no 'truncated' emission and the event is showered from the scale of the hardest emission.
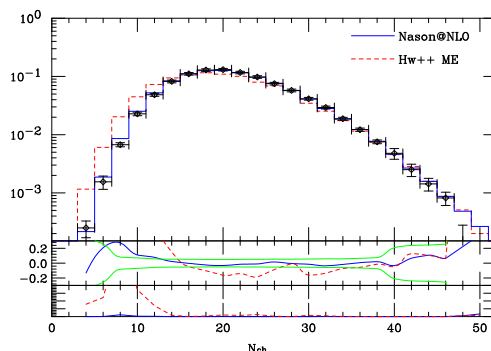
Figure 6: The distribution of the charged particle multiplicity. Data from the OPAL experiment at LEP [11].

v) If there is a 'truncated' emission, the next step is to determine the transverse momentum p_T^t of the emission. This is given by [6]

$$p_T^t = \sqrt{(1 - z_t)^2(\tilde{q}^2 - \mu^2) - z_t Q_g{}^2} \ .$$ (3.7)

If $p_T^t{}^2 < 0$ or $p_T^t > p_T$ go to step ii).

vi) We now have values for z_t, the momentum fraction of the quark after the first emission, p_T^t, the transverse momentum of the first emission, z, the momentum fraction of the hardest emission and p_T, the transverse momentum of the hardest emission. This is illustrated in figure 5. We can then reconstruct the momenta of the partons as described in [6]. The orientation of the quark, antiquark and hardest emission with respect to the beam axis is determined as explained there for the hard matrix element correction.

In principle this procedure could be iterated to generate a multi-gluon truncated shower. However, for the present, we consider only the effect of at most one extra gluon emission. As discussed in [4], the initial showering scale of the hardest gluon is set equal to the showering scale of the quark or antiquark closest in angle to it. This gives the right amount of soft radiation colour connected to the gluon line.

4. Results and data comparisons

One million events were generated as described above and then interfaced with the SMC, `Herwig++`. 13% of the events acquired an extra 'truncated' gluon. A p_T veto was imposed on the subsequent shower starting from the hardest emission to the hadronization scale which was tuned to 0.4 GeV. Table 1 and figure 6 show respectively the average multiplicities of a wide range of hadron species and the charged particle multiplicity distribution. The subsequent figures are plots of comparisons with event shape distributions from the DELPHI experiment at LEP [8].
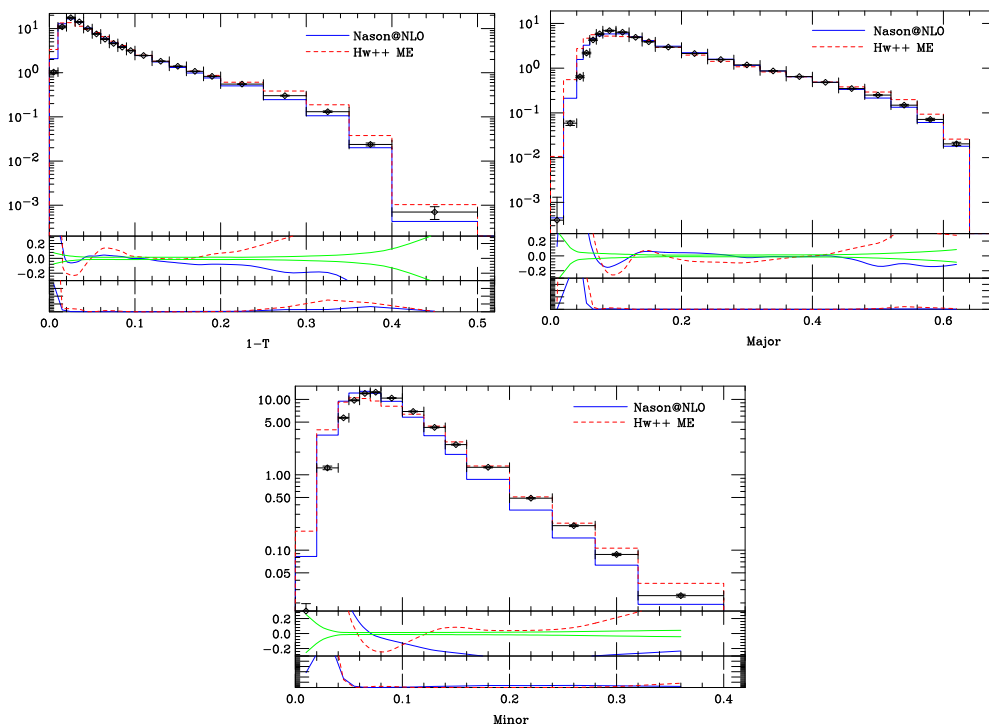
– 10 –

Figure 7: Thrust, Thrust major and Thrust minor. Data from the DELPHI experiment at LEP [8].

The upper panel below the main histograms shows the ratio $\frac{M_i - D_i}{D_i}$ (where M_i and D_i stand for Monte Carlo result and data value respectively) compared with the relative experimental error (green). The lower panel shows the relative contribution to the χ^2 of each observable. As in [6], the χ^2 contributions allow for a 5% uncertainty in the predictions if the data are more accurate than this. Finally, in table 2 we show a list of χ^2 values for all observables that were studied during the analysis. The results were generated using `Herwig++` 2.0 [9] which includes some improvements in the simulation of the shower and hadronization as described in [9] leading to some changes in the χ^2 for specific observables relative to [6], although in most cases the changes are small.

5. Conclusions

We have successfully implemented the Nason method of generating the hardest emission first and subsequently adding a truncated shower for e^+e^- annihilation into hadrons.

We have tested the method against data from e^+e^- colliders and for almost all examined observables, the simulation of the data is improved with respect to `Herwig++`. In particular the Nason method seems to fit the data better in the soft regions of phase space. The poorer fits obtained for variables such as the thrust minor which vanish in the three-jet limit (and in general for planar events) may be attributable to the lack of multiple emission in the truncated shower.
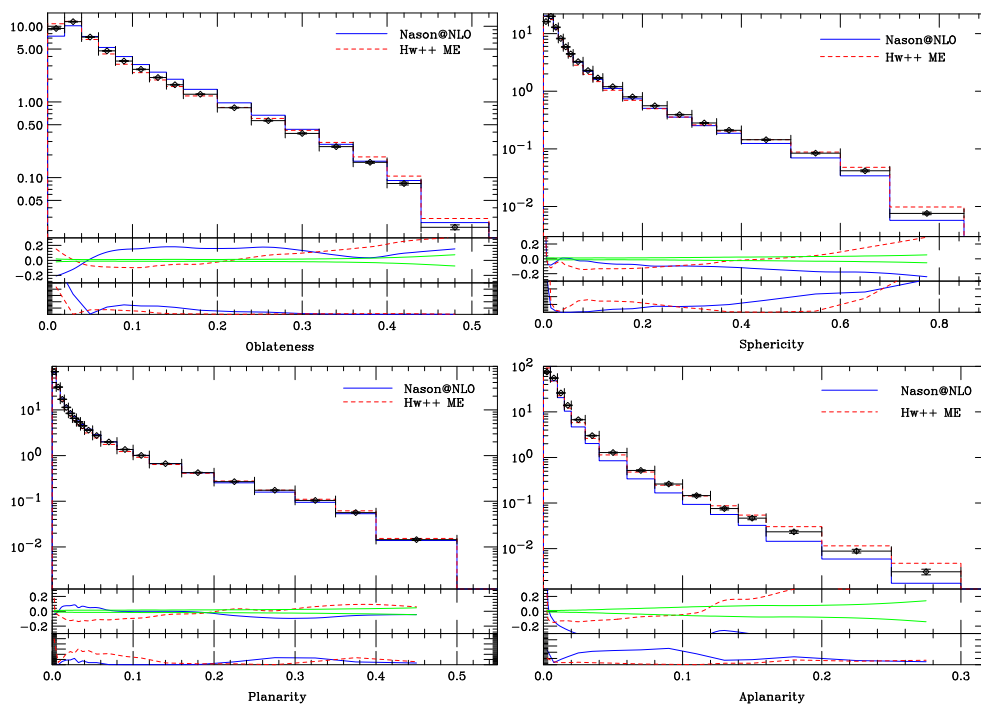
Figure 8: Oblateness, Sphericity, Aplanarity and Planarity distributions. Data from the DELPHI experiment at LEP [8].
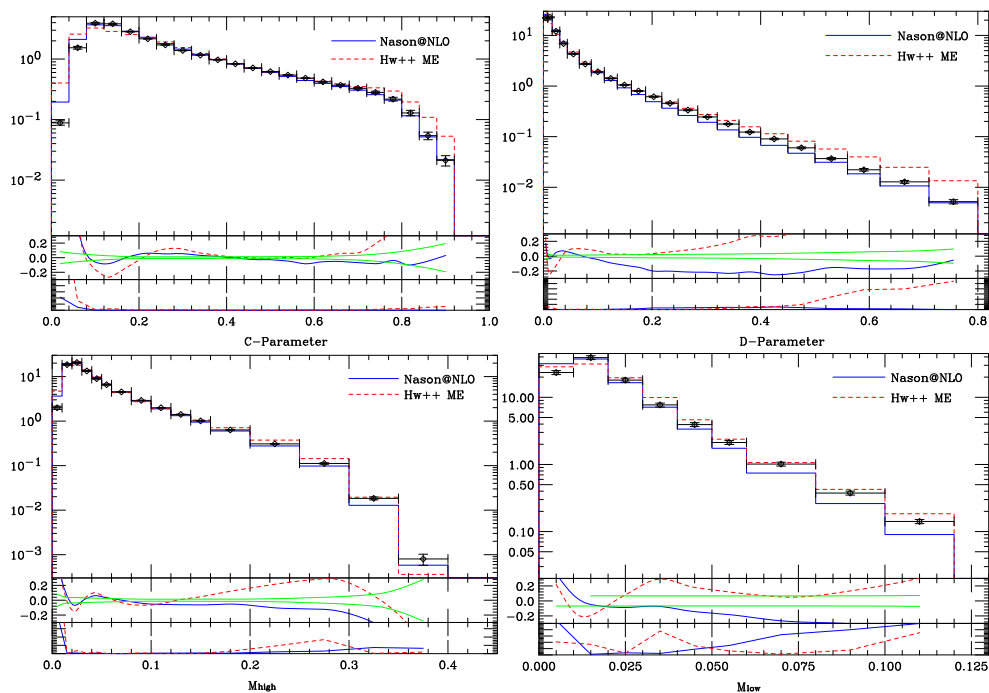

Figure 9: C Parameter and D Parameter distributions and the high, M_{high} and low, M_{low} hemisphere masses. Data from the DELPHI experiment at LEP [8].
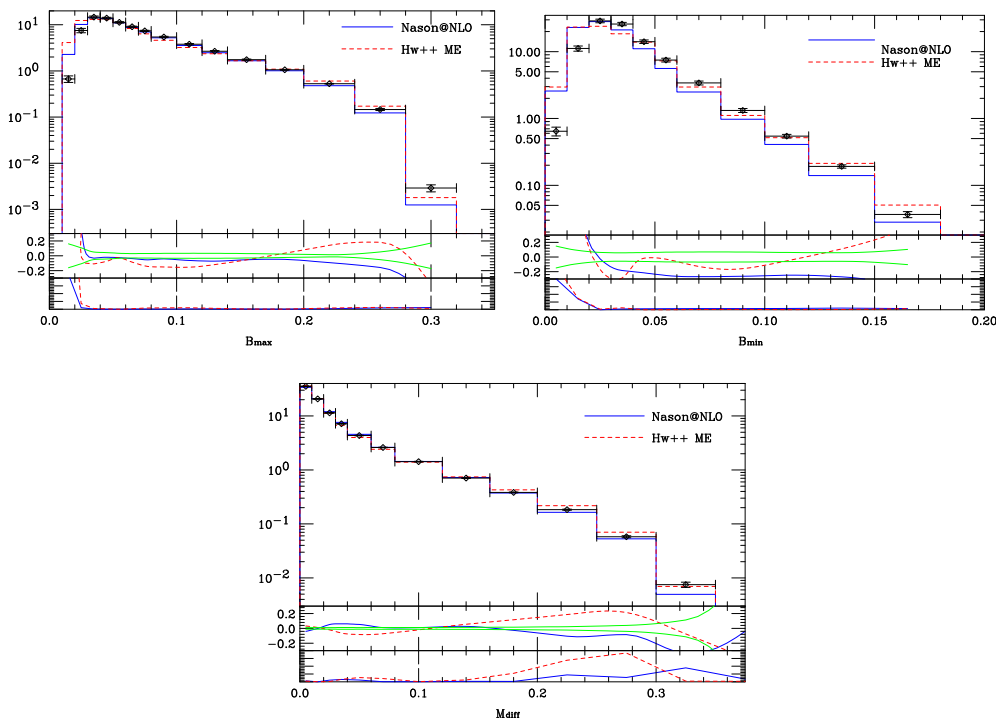
Figure 10: The wide and narrow jet broadening measures $B_{\max}$ and $B_{\min}$ and the difference in hemisphere masses, M_{diff}. Data from the DELPHI experiment at LEP [8].
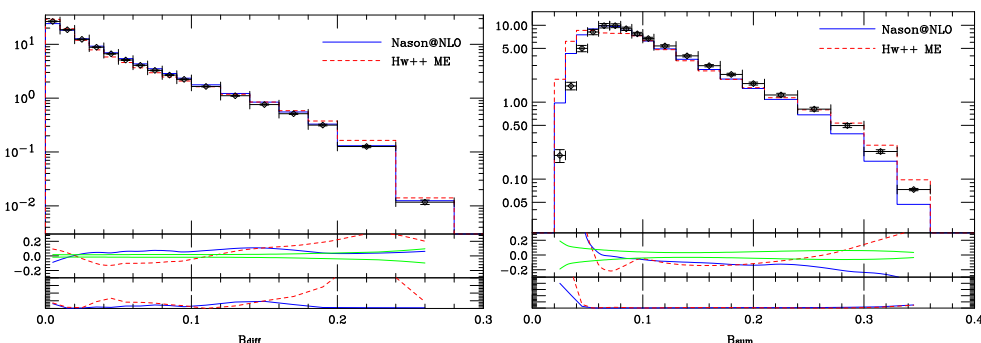

Figure 11: The difference and sum of jet broadenings B_{diff} and B_{sum}. Data from the DELPHI experiment at LEP [8].

The fits are summarized in the χ^2 values shown in table 2. In table 2 we also present the χ^2 values for the observables obtained without the implementation of the 'truncated' shower. We see there is a general improvement in the fits associated with the addition of the 'truncated' emissions.

Future work in this area will extend this method to processes with initial state radiation in hadron-hadron collisions aiming at simulating Tevatron and LHC events.

Observable	Herwig++ ME	Nason@NLO with truncated shower	Nason@NLO w/o truncated shower
$1 - T$	36.52	9.03	9.81
Thrust Major	267.22	36.44	37.65
Thrust Minor	190.25	86.30	90.59
Oblateness	7.58	6.86	6.28
Sphericity	9.61	7.55	9.01
Aplanarity	8.70	22.96	25.33
Planarity	2.14	1.19	1.45
C Parameter	96.69	10.50	11.14
D Parameter	84.86	8.89	10.88
M_{high}	14.70	5.31	6.61
M_{low}	7.82	12.90	13.44
M_{diff}	5.11	1.89	2.09
B_{max}	39.50	11.42	12.17
B_{min}	45.96	35.2	36.16
B_{sum}	91.03	28.83	30.58
B_{diff}	8.94	1.40	1.14
N_{ch}	43.33	1.58	10.08
$\langle \chi^2 \rangle$/bin	56.47	16.96	18.49

Table 2: χ^2/bin for all observables we studied.

Acknowledgements

References

[1] S. Frixione and B.R. Webber, *Matching NLO QCD computations and parton shower simulations*, *JHEP* **06** (2002) 029 [hep-ph/0204244].

[2] S. Frixione, P.Nason and B.R. Webber, *Matching NLO QCD and parton showers in heavy flavour production*, *JHEP* **08** (2003) 007 [hep-ph/0305252].

[3] S. Frixione and B.R. Webber, *The MC@NLO 3.3 event generator*, hep-ph/0612272.

[4] P. Nason, *A new method for combining NLO QCD with shower monte carlo algorithms*, *JHEP* **11** (2004) 040 [hep-ph/0409146].

[5] P. Nason and G. Ridolfi, *A positive-weight next-to-leading-order Monte Carlo for Z pair hadroproduction*, *JHEP* **08** (2006) 077 [hep-ph/0606275].

[6] S. Gieseke, A. Ribon, M.H. Seymour, P. Stephens and B. Webber, *Herwig++ 1.0: an event generator for e^+e^- annihilation*, *JHEP* **02** (2004) 005 [hep-ph/0311208].

[7] S. Gieseke, P. Stephens and B. Webber, *New formalism for QCD parton showers*, *JHEP* **12** (2003) 045 [hep-ph/0310083].

[8] DELPHI collaboration, P. Abreu et al., *Tuning and test of fragmentation models based on identified particles and precision event shape data*, *Z. Physik* **C 73** (1996) 11.

[9] S. Gieseke et al., *Herwig++ 2.0 release note*, `hep-ph/0609306`.

[10] B.R. Webber, *Fragmentation and hadronization*, `hep-ph/9912292`.

[11] OPAL collaboration, P.D. Acton et al., *A study of charged particle multiplicities in hadronic decays of the Z0*, *Z. Physik* **C 53** (1992) 539.